

# The Theory of Critical Distances to predict Static Failures in Notched Brittle Components subjected to Multiaxial Loading

F. Pessot<sup>1</sup>, L. Susmel<sup>2,3</sup>, D. Taylor<sup>3</sup>

<sup>1</sup>Department of Mechanical Engineering, University of Udine, Via delle Scienze, 208 – 33100 Udine, Italy. E-mail: [federico.pessot@virgilio.it](mailto:federico.pessot@virgilio.it)

<sup>2</sup>Department of Engineering, University of Ferrara, Via Saragat, 1 – 44100 Ferrara, Italy. E-mail: [ssl@unife.it](mailto:ssl@unife.it)

<sup>3</sup>Department of Mechanical Engineering, Trinity College, Dublin 2, Ireland. E-mail: [dtaylor@tcd.ie](mailto:dtaylor@tcd.ie)

**ABSTRACT.** *This paper summarises an attempt to use the Theory of Critical Distances (TCD) to predict static failures in notched brittle components when the applied system of forces results in multiaxial stress states in the vicinity of the stress concentrator apex. In order to reformulate the TCD to coherently address this complex problem, the cracking behaviour of cylindrical specimens of PMMA, weakened by different geometrical features and tested under combined tension and torsion, were initially investigated. The direct inspection of the cracked specimens showed that, in an incipient failure condition, the cracking mechanisms changed as the degree of multiaxiality of the stress field damaging the material process zone changed; this held true even though, from an engineering point of view, the investigated material showed a classical brittle behaviour (that is, Mode I dominated). In more detail, in tension (and in plain-specimen torsion) failure occurred as soon as a small craze/crack initiated. On the contrary, for notched specimens in torsion failure was preceded by the formation and growth of many small cracks near the notch root. This complex material cracking behaviour resulted in values of the material characteristic length which changed as the degree of multiaxiality of the stress field damaging the material in the vicinity of the stress raiser apex changed. The above phenomena were incorporated into the devised reformulation of the TCD, allowing our method to perform predictions falling in an error interval of about 15%. This result is very interesting, especially in the light of the fact that the TCD can easily be used to post-process linear-elastic FE models, making it suitable for being successfully employed in an industrial reality.*

## INTRODUCTION

In the recent years, Taylor has extended the use of the TCD from the high-cycle fatigue [1, 2] to the static field showing that this approach can successfully be used also to predict static failures in brittle (or quasi-brittle) materials weakened by any kind of geometrical feature (that is, short, sharp and blunt notches) [3-5]. To use this method in

situations of practical interest, it is useful to remember here that the TCD can be formalised in different ways [1]. In particular, the equivalent stress to be directly compared to the inherent material strength,  $\sigma_0$ , can be calculated at a certain distance from the notch tip (Point Method, PM), can be averaged over a line (Line Method, LM), over an area (Area Method, AM) or, finally, it can be averaged in a finite volume (Volume Method, VM).

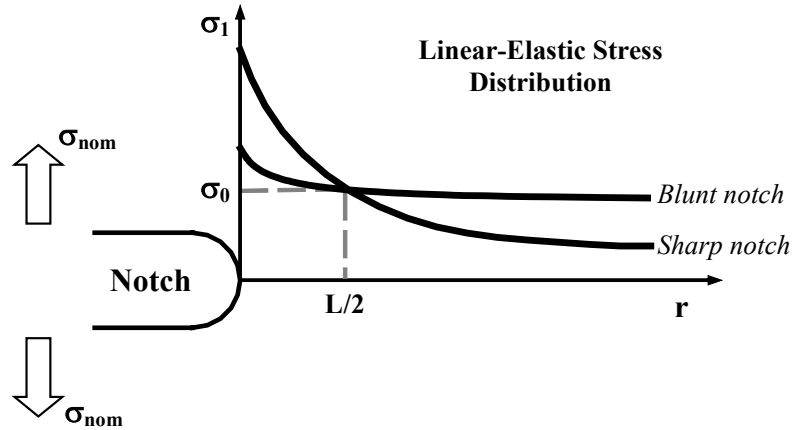


Figure 1. Notched component subjected to a remote uniaxial nominal stress and stress-distance curves due to two notches having different sharpness.

In particular, under uniaxial fatigue loading the PM (that is, the simplest formalisation of the TCD) postulates that the structural integrity of the assessed component is not in a critical condition as long as the maximum principal stress, calculated at a distance from the notch tip equal to  $L/2$ , is lower than the inherent material strength,  $\sigma_0$  (Fig. 1). Here  $L$  is the so-called material characteristic length, i.e. a mechanical property different for different materials, which is defined as follows:

$$L = \frac{1}{\pi} \left( \frac{K_{Ic}}{\sigma_0} \right)^2 \quad (1)$$

In the above definition,  $K_{Ic}$  is the plane strain material toughness, whereas the inherent strength parameter changes as the type of the considered material changes. To be precise, in brittle materials, like in ceramics [3],  $\sigma_0$  is equal to the ultimate tensile stress,  $\sigma_{UTS}$ , whereas when static failures are preceded by a certain amount of plasticity (quasi-brittle behaviour),  $\sigma_0$  takes on a value which is higher than the plain material strength and it can be determined only carrying out ad-hoc experimental investigations [4, 5]. For the sake of simplicity, the latter way of determining the inherent material strength is briefly sketched in Fig. 1: the critical distance,  $L/2$ , and  $\sigma_0$  result from the intersection of the linear-elastic stress-distance curves determined in incipient failure condition and generated by testing two specimens weakened by blunt and sharp notches, respectively.

The need for employing such a procedure is due to the fact that, to properly apply the TCD,  $K_{Ic}$  and  $\sigma_0$  have to be determined considering defect-free materials. On the contrary, the conventional manufacturing techniques result in materials containing micro-defects which, in many cases, affect the material strength: several commercial engineering materials show a  $\sigma_{UTS}$  value lower than their inherent strength,  $\sigma_0$ . It is interesting to point out that this problem was extensively investigated by Taylor and co-workers when applying the TCD to predict static failures in notched specimens of polymethylmethacrylate (PMMA) [4]. Furthermore, they showed that the TCD could be successfully employed to estimate PMMA's static strength as long as the stress concentration factor,  $K_t$ , of the assessed component is larger than the ratio between the inherent and the ultimate tensile strength [4].

## EXPERIMENTAL DETAILS

The material employed in the present study was a commercial PMMA supplied in cylindrical bars. Plain and notched specimens were tested under tension/torsion by using an INSTRON 8874 biaxial servohydraulic testing machine.

Four different cylindrical geometries were machined: the tested V-notched specimens had gross diameter equal to 12.8mm, net diameter to 8.2mm, notch opening angle equal to  $60^\circ$  and notch root radii equal to 0.2mm, 0.4mm, 1.2mm and 4.0mm, respectively. Moreover, in order to determine the critical distance value as well as the inherent material strength under plane stress condition, two different notched flat specimens were machined starting from the same parent material as the one used to machine the cylindrical specimens. Such flat specimens were weakened by V-notches and they had thickness equal to 0.75mm, gross width to 12.8mm, net width to 8.2mm, notch opening angle to  $60^\circ$  and notch root radii equal to 0.2mm and 0.4mm, respectively.

Finally, it is interesting to highlight that, and according to the Maximum Principal Stress Theory, the experimental values of the ultimate strength under both tension and torsion were equal to 67 MPa.

## MATERIAL CRACKING BEHAVIOUR

In order to coherently reformulate the PM to make it suitable for predicting static failures in notched brittle components under multiaxial loading, several tests were initially carried out to deeply investigate the material cracking behaviour in the presence of stress concentration phenomena. In particular, cylindrical V-notched specimens having notch root radius equal to 0.2mm were tested under both tension, torsion and combined loading (with a ratio between the applied nominal tensile and torsional stress equal to 0.55).

Under uniaxial loading, the behaviour showed by the tested PMMA was the typical one of a brittle material: the load vs. displacement curve was perfectly linear up to the complete failure (Fig. 2a) and the specimens broke due to Mode I cracks initiated at a material superficial defect (in Fig. 2b the crack initiation site is pointed out by the

arrow). In other words, in tension (both in plain- and notched-specimens) and in plain-specimen torsion final failures were caused by the initiation of a small craze/crack.

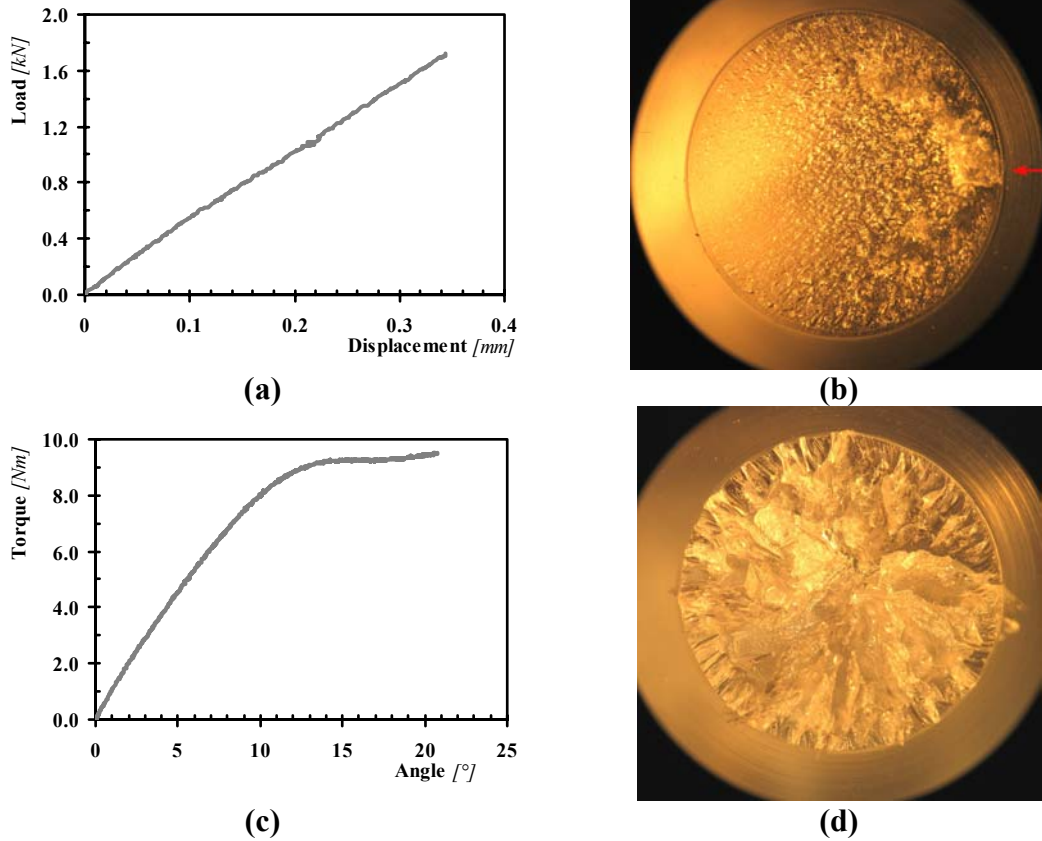


Figure 2. Load vs. displacement curve (a) and cracked surface (b) under tension; torque vs. angle curve (b) under torsion (notched specimen) and resulting fracture surface after failure (c).

On the contrary, the material cracking behaviour showed by the notched specimens loaded in torsion was seen to be much more complex. In particular, the torque vs. angle curves were characterised by an initial linear-elastic stretch followed by an almost horizontal plateau preceding the final fracture (Fig. 2c). The specimen failure was seen to be caused by multiple Mode I cracks resulting in the classical “factory roof” surface (Fig. 2d). In order to better investigate this complex scenario trying, at the same time, to explain the presence of the horizontal plateau in the torsional stress vs. shear strain curves, some loading-unloading tests were carried out. These tests showed that failures under torsion were preceded by the formation and growth of many small cracks near the notch root (Fig. 3). These cracks formed on planes perpendicular to the maximum principal stress (i.e. at 45° to the specimen axis) and final failure occurred by the linking together of many of these small cracks. All these micro-cracks while propagating interacted with each other retarding the final failure by dissipating energy. This fact

resulted in stress vs. strain torsional curves characterised by the above mentioned horizontal plateau preceding the final breakage.

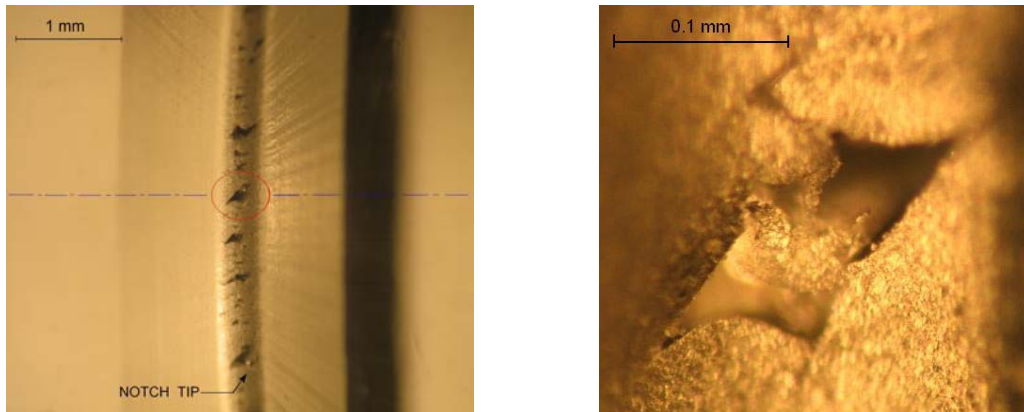


Figure 3. Initiation and growth of small cracks near the notch root under torsion.

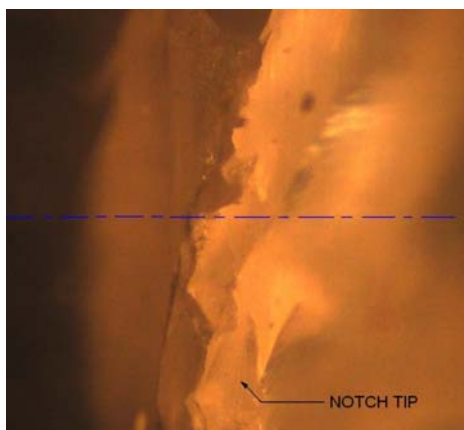


Figure 4. Small tensile crack under combined tension/torsion (magnification 250X).

Finally, under combined tension-torsion the material cracking behaviour was seen to be in between the two extreme conditions discussed above. In particular, the observed Mode I cracks preceding the final failure were always perpendicular to the maximum principal stress (Fig. 4), but the number of small cracks due to the coalescence phenomenon resulting in the final failure was seen to decrease as the tensile stress contribution to final failure increased, disappearing under uniaxial loading.

## THE TCD TO PREDICT STATIC FAILURES IN NOTCHED BRITTLE MATERIALS UNDER MULTIAXIAL LOADING

According to the observed material cracking behaviour and to coherently extend the use of the PM to multiaxial situations, the following initial hypotheses were formed:

- 1) In terms of maximum principal stress, the inherent material strength under tension is equal to its value under torsion;
- 2) Failures are caused by the propagation of small tensile cracks, whose initiation depends on the maximum principal stress,  $\sigma_1$ ;
- 3) The critical distance value changes as the degree of multiaxiality of the stress field in the vicinity of the stress raiser apex changes.

It is interesting to highlight that the first hypothesis was directly derived from the experimental finding that the measured ultimate stress in tension was seen to be equal to its value under pure torsional loading: i.e. the material exhibits classic brittle behaviour. Due to the fact that the material cracking behaviour was seen to be Mode I governed, the maximum together with the minimum principal stress were used to introduce the following ratio suitable for defining the degree of multiaxiality of the stress field damaging the material in the vicinity of the notch tip:

$$\rho = -\frac{\sigma_3}{\sigma_1} \quad (2)$$

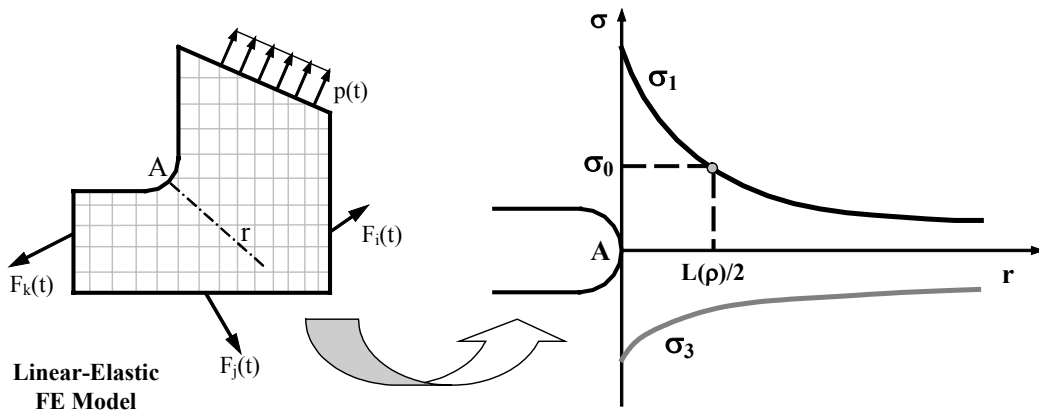


Figure 5. Procedure for the in field application of the proposed method.

In particular, it is trivial to observe that under plane stress Mode I loading  $\rho$  is equal to zero, whereas under Mode III loading it is equal to unity.

Finally, by using the  $\rho$  ratio to measure the complexity of the stress field close to the notch tip, the third hypothesis was formalised as follows:

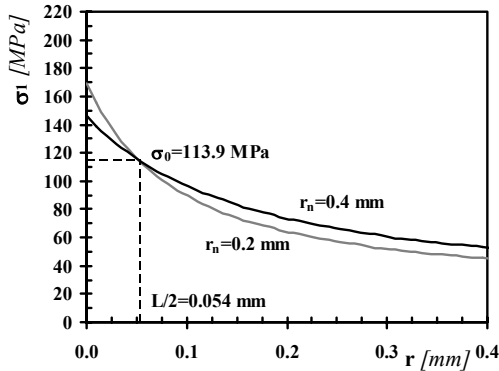
$$L(\rho) = a \cdot \rho + b \quad (3)$$

where  $a$  and  $b$  are material constants to be determined by considering the critical distance generated under two different values of the  $\rho$  ratio. For instance, Eq. (3) could easily be calibrated by considering the material characteristic length generated both under plane stress Mode I loading ( $\rho=0$ ) and under Mode III loading ( $\rho=1$ ).

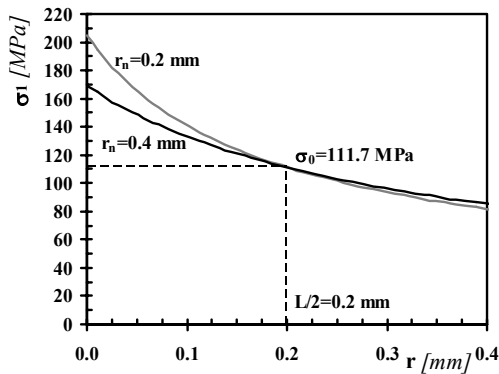
The procedure for the in field application of the devised multiaxial PM is sketched in Fig. 5. In particular, after locating the position of a potential crack initiation point on the component surface (Point A in Fig. 5), by using either numerical or analytical approaches, it is possible to define the linear-elastic stress distribution (plotted in terms of both  $\sigma_1$  and  $\sigma_3$ ) along the focus path (the focus path is a straight line perpendicular to the surface and emanating from the crack initiation point - see Fig. 5). At any distance,  $r$ , from the crack initiation site it is possible now to calculate the corresponding  $\rho$  ratio and, from Eq. (3), the resulting value of  $L(\rho)$ . The value of the critical distance,  $L(\rho)/2$ ,

to be used for predicting the material strength in terms of the proposed multiaxial PM is the one assuring the following trivial condition:

$$\frac{L(\rho)}{2} - r = 0 \Rightarrow \frac{(a \cdot \rho + b)}{2} - r = 0 \quad (4)$$



(a)



(b)

Figure 6.  $L/2$  and  $\sigma_0$  determined both under plane stress Mode I loading (a) and under Mode III loading (b).

The stress-distance curves generated testing V-notches having notch root radius,  $r_n$ , equal to 0.2mm and 0.4mm, respectively, are plotted in Fig. 6. These diagrams show that under plane stress Mode I loading, the applied procedure resulted in a critical distance value,  $L/2$ , equal to 0.054mm and in an inherent material strength,  $\sigma_0$ , equal to 113.9 MPa (Fig. 6a), on the contrary, under Mode III loading  $L/2$  was equal to 0.2mm and  $\sigma_0$  equal to 111.7 MPa (Fig. 6b). It is interesting to observe that the above values were in perfect agreement with hypothesis 1) and 3): the complexity of the stress field damaging the material process zone influenced the value of  $L/2$ , but not the value of the inherent material strength. According to the above experimental results, constants  $a$  and

According to the devised method, failure in a notched brittle component occurs when, at a distance from the notch tip equal to the value given by Eq. (4), the maximum principal stress,  $\sigma_1$ , equals the inherent material strength,  $\sigma_0$ .

## METHOD VALIDATION BY EXPERIMENTAL DATA

In order to check accuracy and reliability of the devised extension of the PM, the notched cylindrical specimens of PMMA were tested under pure tension, under pure torsion and under combined tension-torsion. In particular, for the biaxial tests three different ratios between nominal tensile and torsional stress were considered:  $\sigma_{nom}/\tau_{nom}$  equal to 1.00, 0.55 and 0.23, respectively.

Following the procedure sketched in Fig. 1, the critical distance value,  $L/2$ , and the inherent material strength,  $\sigma_0$ , were determined by means of some calibrations results generated both under Mode I loading (by testing the V-notched flat specimens) and under Mode III loading.

b in Eq. (3) were equal to 0.292 and to 0.108, respectively, and the average value of  $\sigma_0$  equal to 112.8 MPa.

Table 1 summarises the accuracy obtained applying the multiaxial PM to the generated results. This Table shows that predictions were in general highly accurate. Only the predictions performed considering specimens having notch root radius,  $r_n$ , equal to 4.0mm were characterised by errors higher than 20%: this fact was not surprising at all, because, as clearly highlighted by Taylor and co-workers in Ref. [4], due to the low value of  $K_t$ , those specimens were out of the range of validity of our theory. Finally, it is interesting to highlight that a high accuracy level was also obtained when predicting the strength of the cylindrical notched specimens loaded in pure tension, even though, due to the axisymmetry of the specimens, the stress fields along the notch bisectors were characterised by negative values of  $\rho$ .

Table 1. TCD accuracy in predicting failures in the tested notched specimens.

$\sigma_{nom}/\tau_{nom}$	Error (%)			
	$r_n=0.2mm$	$r_n=0.4mm$	$r_n=1.2mm$	$r_n=4.0mm$
$\infty$	-16.4	-11.9	9.6	46.6
1.00	-8.4	-9.8	4.2	-2.3
0.55	-18.6	-12.8	1.4	10.2
0.23	-6	-1.8	10.6	23.1
0	0	0	19.7	40.6

## CONCLUSIONS

The proposed extension of the TCD to multiaxial situations was seen to be successful allowing predictions to fall within an error interval of about 15%. This results is very interesting, especially in the light of the fact that our method can be used to post-process linear-elastic FE results, making it suitable for being used to assess real components in situations of practical interest.

## REFERENCES

1. Taylor, D. (1999) *Int. J. Fatigue* **21**, 413-420.
2. Taylor, D. (2005) *Eng. Fail. Anal.* **12**, 906-914.
3. Taylor, D. (2004) *Eng. Frac. Mech.* **71**, 2407-2416.
4. Taylor, D., Merlo, M., Pegley R., Cavatorta, M. P. (2004) *Material Science and Engineering A* **382**, 288-294
5. Taylor, D., Cornetti, P., Pugno N. (2005) *Eng. Frac. Mech.* **72**, 1021-1038.